Journal of Cleaner Production 350 (2022) 131339

Contents lists available at ScienceDirect

Journal of Cleaner Production

journal homepage: www.elsevier.com/locate/jclepro

Decarbonizing primary steel production : Techno-economic assessment of a hydrogen based green steel production plant in Norway

Abhinav Bhaskar *, Rockey Abhishek, Mohsen Assadi, Homam Nikpey Somehesaraei

University of Stavanger, 4036, Norway

ARTICLE INFO

Handling Editor: Kathleen Aviso

Keywords:
Industrial decarbonization
Hydrogen direct reduction
Water electrolysis
Green steel
Climate change
Norway
Optimization
Day ahead electricity market

ABSTRACT

High electricity cost is the biggest challenge faced by the steel industry in transitioning to hydrogen based steelmaking. A steel plant in Norway could have access to cheap, emission free electricity, high-quality iron ore, skilled manpower, and the European market. An open-source model for conducting techno-economic assessment of a hydrogen based steel manufacturing plant, operating in Norway has been developed in this work. Levelized cost of production (LCOP) for two plant configurations; one procuring electricity at a fixed price, and the other procuring electricity from the day-ahead electricity markets, with different electrolyzer capacity were analyzed. LCOP varied from $622/tls to $722/tls for the different plant configurations. Procuring electricity from the day-ahead electricity markets could reduce the LCOP by 15%. Increasing the electrolyzer capacity reduced the operational costs, but increased the capital investments, reducing the overall advantage. Sensitivity analysis revealed that electricity price and iron ore price are the major contributors to uncertainty for configurations with fixed electricity prices. For configurations with higher electrolyzer capacity, changes in the iron ore price and parameters related to capital investment were found to affect the LCOP significantly.

1. Introduction

The Inter-governmental panel on climate change(IPCC) has estimated that the total human contribution to global surface temperature increase is in the range of 0.8 °C–1.3 °C, with a best estimate of 1.07 °C (V et al., 2021). The evidence for human-induced climate change affecting the extreme weather events such as heatwaves, heavy precipitation, droughts, tropical cyclones, and in particular their attribution to human influence has strengthened. High concentration of greenhouse gases such as carbon dioxide, methane, nitrous and nitrogen oxides, halogenated gases and volatile organic compounds in the atmosphere are the main contributors to the increased radiative forcing and consequent rise in global mean surface temperatures. Rapid decarbonization of all sectors of the economy is imperative to limit the global mean surface temperature increase to 1.5 °C by the end of the century (Fischedick et al., 2014).

Approximately 1.86 billion tonnes of crude steel were produced in 2019 (Worldsteel, 2020). Production of 1.34 billion tons of steel, with an average emission of 1.8 tCO_2/tls, contributed 2.4 $GtCO_2$ emissions in 2019, which corresponds to 7% of the global energy related CO_2 emissions (IEA, 2021). While improved material efficiency, product service life extension, increased share of recycling and material substitution are viable measures to reduce steel demand, and hence the associated emissions, steel demand is likely to increase in the short and medium term (IEA, 2020). Incremental efficiency improvements are likely to contribute to emission reduction but would not be sufficient in meeting the emission reduction targets required to meet the goals of the Paris climate agreement (Rissman et al., 2020).

Introduction of alternative production technologies with zero carbon-footprint would be essential to decarbonize the iron and steel sector (Åhman et al., 2018). Mitigation technologies can be broadly divided in carbon capture utilization and storage or carbon direct avoidance technologies. The former aim to capture the CO_2, and either utilize it, or store it in geological reservoirs. Portho et al. identified three main alternatives for the utilization of off-gases in the steelmaking plant i.e. use for thermal energy, recovery of valuable compounds for selling and the synthesis of a high-added value product (Uribe-Soto et al., 2017). Through the Carbon2chem project, thyssenkrupp aims to use the top gases from the blast furnace at Duisburg, Germany to produce value added chemicals like methanol and higher alcohols (Wich et al., 2020). The project consortium includes chemical companies and industrial research institutes. Arcelor Mittal, another leading steel manufacturer aims to use the off-gases produced at its steel plant in Ghent, Belgium to produce 63,000 tonnes of ethanol per year (Birat, 2020).

With carbon direct avoidance technologies, the focus has been on technologies which can replace coke as the reducing agent (Fischedick

* Corresponding author.
E-mail address: abhinav.bhaskar@uis.no (A. Bhaskar).

https://doi.org/10.1016/j.jclepro.2022.131339
Received 27 September 2021; Received in revised form 8 March 2022; Accepted 11 March 2022
Available online 25 March 2022

et al., 2014). While a combination of CO and H_2 have been used since the 1970's for the direct reduction of iron ore, there has been interest in the use of electricity for reducing iron oxide, similar to the electrolysis of Alumina. Both high-temperature and low-temperature electrolysis pathways are being explored, but are currently at low technology readiness levels, and are constrained by the use of expensive catalysts (Bailera et al., 2021).

Hydrogen can replace coke as a reducing agent in a hydrogen direct reduction shaft furnace (H_2-SF) (da Costa et al., 2013). The resulting direct reduced iron (DRI) can be fed to an electric arc furnace (EAF) for the production of emission free steel. Weigel et al. (2016) conducted a multi-criteria analysis of four mitigation technologies, and found H_2-SF-EAF route for primary steel production to be the most competitive. Use of hydrogen in existing blast furnaces has also been studied by some researchers. Suer et al. (2021) analyzed the injection of natural gas or hydrogen into a blast furnace, addition of hot briquetted iron (HBI) into the blast furnace produced from direct reduction of iron ore using natural gas-based and use of 100% hydrogen in BF. Their analysis revealed that the use of HBI into a blast furnace is a reasonable way to reduce emissions in the short and medium term, and will allow the creation of the hydrogen market till the metallurgical challenges of H_2-SF-EAF based method are completely resolved. Vogl et al. (2018) conducted techno-economic assessment of a H_2-SF-EAF system powered by grid electricity, and found that hydrogen based steel production could be cost competitive with a BF-BOF based plant at an emission price in the range of €34 to €68/tCO_2, and at an electricity price of €40/MWh. Krüger et al. (2020) studied the integration of low and high temperature electrolyzers with the H_2-SF-EAF process, and found that high temperature electrolyzers could lower the specific energy consumption. Jacobasch et al. (2021) evaluated the economic feasibility of a hydrogen direct reduction steel plant, and calculated the carbon mitigation cost. Hydrogen production from three different electrolyzer technologies i.e. alkaline, proton electron membrane and solid oxide electrolysis was considered. They calculated the CO_2 mitigation cost to be 89 €/t. To alleviate the problems of storing large quantities of hydrogen, where geological storage sites are hard to find, hydrogen carriers could be used. Andersson (2021) evaluated the integration of four different hydrogen carriers for in the steelmaking process. They were compared based on their thermodynamic and economic data to estimate operational and capital costs. Methanol was found to be the most promising alternative.

Steel manufacturers have announced multiple projects to explore the technical and commercial feasibility of hydrogen based steelmaking. Under the HYBRIT project in Sweden, various aspects of the hydrogen based steelmaking's value chain are being tested. A pilot plant running on 100% hydrogen as reducing gas was commissioned in August, 2020 (Pei et al., 2020). Other aspects of the value chain such as hydrogen storage in rock caverns, production of emission free pellets etc. are also being explored. A hydrogen-based fine-ore reduction (HYFOR) pilot plant developed by Primetals Technologies was commissioned in Donawitz, Austria in April, 2021. The HYFOR technology could enable the use of iron ore fines in the direct reduction process, which could reduce the operatiing costs (Primemetals, 2022). Green steel tracker is an open-source database to track the recent development in the decarbonization of the iron and steel industry (Vogl et al., 2021b). The project database shows that hydrogen based steelmaking is increasingly becoming the technology of choice for decarbonizing, among the largest steelmakers i.e. Baowu steel, Arcelor Mittal, thyssenkrupp, Tata steel, Posco etc. New entrants in the steel sector, such as H2green steel in Sweden, plan to use hydrogen based steelmaking. It has plans to produce five million tons of green steel by 2030 (Vogl et al., 2021a).

1.1. Research context

Approximately 60 kg of hydrogen is required for the production of one ton of steel (Bhaskar et al., 2021). Hydrogen is currently produced from fossil fuels, which results in significant emissions (Howarth and Jacobson, 2021). In order to use hydrogen for decarbonizing the industry, zero emission hydrogen production technologies such as water electrolysis need to be considered. Water electrolysis is an energy intensive process, and availability of low cost electricity is a necessary condition for producing cost competitive H_2-SF-EAF based steel. This creates an opportunity to produce hydrogen at locations with low electricity prices, and high renewable energy potential (IRENA, 2022). Gielen et al. found that the relocation of iron and steel industry to regions with high renewable potential could increase renewable energy deployment, and create more value through sustainable industrial activities in resource-rich countries (Gielen et al., 2020). Bataille et al. analyzed the economic feasibility of producing Hydrogen based DRI in South Africa, and found that primary iron production with hydrogen could increase value added from local iron ore and solar energy resources, increase exports and initiate transformation to a more sustainable industry (Trollip et al., 2022).

Norway has one of the lowest wholesale electricity price and energy tax rates in Europe, and has a low grid emission factor, as majority of the electricity is supplied by hydroelectric power plants (Moro and Lonza, 2018). Many energy intensive manufacturing industries such as paper and pulp, ferro-alloys and non-ferrous metals (Aluminum) are operational in Norway. Almost one-third of Norway's total electricity was used by energy intensive industries in 2019. More than 60% of the industrial electricity demand came from the Aluminum industry (Norway, 2021). More recently, low-electricity prices, and high-renewable energy potential of Norway is being leveraged by the ammonia producers to reduce emissions from the ammonia value chain. A collaborative project between Yara, Aker Clean Hydrogen and Statkraft called HEGRA has been announced recently (YARA, 2021). Hydrogen will be produced from water electrolysis, and will decarbonize Yara's ammonia factory on Herøya in Porsgrunn. Notably, the first electricity based hydrogen production plants were commissioned in Norway in 1929, and many leading electrolyzer manufacturers such Nel Hydrogen ASA have manufacturing facilities in Norway (IRENA, 2022). Along with the availability of cheap, emission-free electricity, Norway has an additional advantage of having access to a highly skilled work force from the metallurgical industry. These factors could enable the establishment of a hydrogen based steelmaking industry in Norway. In order to assess this opportunity, techno-economic assessment model of a grid connected H_2-SF-EAF plant in Norway has been developed in this work. The techno-assessment model was developed to provide answers to the following research questions:

1. What are the enabling factors associated with the H_2-SF-EAF based steel production in Norway?
2. What is the levellized cost of hydrogen based steel production in Norway?
3. Which electricity procurement strategy; fixed power purchase agreements or procurement of electricity from day-ahead electricity markets is most cost-efficient?

Rest of the article is structured as follows. The research framework and methodology is presented in Section 2. Results of the analysis are presented in Section 3, followed by a discussion on the monthly and seasonal variation of electricity prices in Section 4. The results are further discussed, and contextualized in Section 5. Conclusions of this study are presented in Section 6.

2. Methodology

The model is based on the techno-economic assessment framework developed by Thomassen et al. for green chemical production technologies at low technology readiness level (Thomassen et al., 2019). First, market assessment for a green steel manufacturing plant in Norway was conducted. In the second step, a conceptual process model of a grid connected H_2-SF-EAF was developed to calculate the material and energy balance across different components. The model was used to calculate the annual energy consumption, emissions and material requirement for a steel plant with an output capacity One Million ton per annum (Mtpa) of liquid steel. In the third step, levellized cost of steel production was calculated for two electricity procurement strategies using discounted cash-flow analysis i.e. fixed electricity price power purchase agreement, and procurement of electricity from day-ahead markets. In the final step, global sensitivity analysis was conducted using the Sobol sensitivity indices based on the global uncertainty in the input parameter values (Sobol, 2001).

Open-source scientific computation software have been used in this work. The Pandas library was used for retrieving, and analyzing tabular data (McKinney, 2010). Numpy, was used for creating arrays and data handling (Walt et al., 2011). Matplotlib was used for data visualization, and creation of plots (Hunter, 2007). The Ipython notebook environment was used to write the python scripts (Perez and Granger, 2007). The optimization model was written in Python, using PYOMO, which is an open-source optimization framework (Sch et al., 2021). The optimization problem was solved using Gurobi (Gruobi, 2021). The Python scripts, and data used for the analysis are available on the Zenodo repository (Bhaskar, 2021). In the following sections, the different steps are detailed further.

2.1. Market assessment

More than 150 Million tons of steel were used in the European Union(EU) in 2019 (EUROFER, 2020). One-third of the demand originates from the construction sector. The automobile and machinery sector are the two other major demand segments. There has been an increased scrutiny of the embodied emissions of buildings and structures, which includes structural steel used in the construction sector. A global coalition of public and private organizations, called the Industrial deep decarbonization initiative (IDDI) was set up recently to stimulate demand for low carbon industrial materials (UNIDO, 2021). The objectives of IDDI include encouraging governments, and the private sector to buy low carbon steel and cement, and to share data and resources to set common standards and targets across member states. The recent announcements to lower the cap in the EU emission trading system, carbon border adjustment taxes, and emphasis on the use of climate-neutral industrial products could result in an increased demand for green steel in the construction sector in the future (Sartor et al., 2022). Leading automobile manufacturers are moving towards green steel. Volvo, which is a leading automobile manufacturer, and steel producer SSAB have signed a collaboration agreement on research, development, serial production and commercialization of the world's first vehicles to be made of hydrogen reduction based steel. Volvo plans to start the production of concept vehicles and components from hydrogen based green steel by 2021 (Volvo, 2021). Similar, plans have been announced by the Mercedes group, which has invested in an upcoming 5 Mtpa steel production facility in Sweden (Schäfer, 2021). Ørsted, a leading wind energy developer has joined the SteelZero global initiative to drive market demand for net-zero emission steel (Stougaard, 2021).

Norway's proximity to the steel demand centers in the EU could result in lower transportation costs for finished steel from the proposed plant. Interestingly, import of iron and steel, cement, ammonia, aluminum and electricity are included in EU's carbon-border adjustment mechanism (UNCTAD, 2021). Low-emission steel produced in Norway could become cost competitive with other exporters such as Russia, China, India etc. which are still reliant on emission-intensive manufacturing processes. Operations at a magnetite iron ore mining facility are set to resume in Northern Norway. Sydvaranger plans to produce magnetite iron ore concentrate from its mining and processing facilities, which could be used as a raw material input for the hydrogen based steel making (Sydvaranger, 2022). Using domestic iron ore could reduce emission footprint from shipping, and hedge against price fluctuations, which have recently plagued the iron and steel industry. Apart from abundant hydro-power resources, Norway has very good wind electricity potential (both onshore and offshore). The theoretical potential of Norway's offshore is close to 12000 TWh/year, although most of it is located in deep waters and hence costlier to exploit (Bosch et al., 2018). The recent 4.5 GW tenders for fixed bottom plants in Sørlige Nordsjø-II, and floating bottom offshore wind projects in Utsira Nord are an example of the new developments in the Norwegian offshore wind industry. Additional renewable generators could reduce the electricity prices, and reduce operational costs for the proposed H_2-SF-EAF plant.

2.2. Conceptual process model

Hydrogen based steel production can be divided into three distinct sub-processes i.e. hot metal (iron) production in the shaft furnace, conversion of iron to steel in the EAF, and the production and storage of reducing agent (hydrogen). Material and energy flows through the different components were calculated for the production of one ton liquid steel. The specific heat and enthalpy of the different species were calculated using the Shomate equation, as described in Eqs. (1) and (2). The coefficients of the Shomate equations were taken from NIST webBook (Chase, 1998). A conceptual model of the system is presented in Fig. 1.

$$C_p^\circ = A + B*t + D*t^2 + D*t^3 + E/t^2 \quad (1)$$

$$H^\circ - H^\circ_{298.15} = A*t + B*t^2/2 + D*t^3/3 + D*t^4/4 - E/t + F - H \quad (2)$$

2.2.1. Hot metal production in SF

The DRI shaft furnace is counter current solid–gas reactor, where the iron ore pellets, at ambient temperature are fed from the top through a hopper. The iron ore pellet stream is depicted by **M1**. It is assumed that the impurity content in the pellets is 5%, and the impurities are composed of Al_2O_3 and SiO_2. In practice other impurities could be present in the iron ore pellets. Composition of the pellets have an impact on reduction kinetics and thermodynamics. Since, there are no gangue separation processes in the SF-EAF process, it is imperative that the impurity content in the pellets is low. The higher purity requirement has an implication on the cost of the iron ore, and DRI pellets are relatively more expensive compared to raw materials used for blast furnace based iron production. The pelletization process uses fossil fuels as a source for thermal energy, and an upstream emission of 56 kg CO2/t of pellets has been assumed in this study (LKAB, 2017). The reducing gas stream, **M4**, composed of 100% hydrogen enters the shaft furnace at a temperature of 900 °C. The SF operates at a pressure of 6–8 Bar (Maggiolino, 2019). Although SF can operate at atmospheric pressure as well, increasing the pressure could have a positive impact on the diffusivity of the reducing gas, and lead to faster kinetics.

Reduction occurs in three steps, where Hematite (Fe_2O_3) is first converted to Magnetite (Fe_3O_4). In subsequent steps, magnetite is converted to Wüstite (FeO), and finally metallic iron (eFe). Kim et al. found that the easy nucleation, and fast diffusion through the iron oxide product layer are the main reasons for the fast reduction kinetics of hematite to Wüstite conversion (Kim et al., 2021). The conversion from Wüstite to metallic iron is an order of magnitude slower due to sluggish mass transport, particularly of the oxygen through the iron layers. The reduction kinetics of is positively correlated with temperature in the range of 800–1000 °C. Increase in kinetics is attributed to the increase

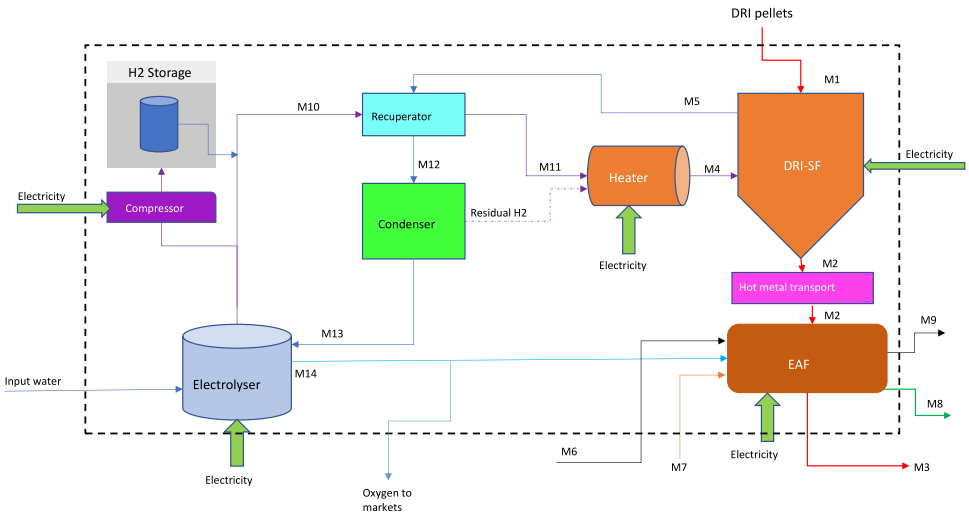

Fig. 1. Schematic of a grid connected H_2-SF-EAF based steel production system.

in diffusivity and reaction rate (Heidari et al., 2021). Reduction kinetics of H_2 was found to be higher than CO, and could result in SF with smaller dimensions (Wagner, 2009). The reduction reaction between hydrogen and iron oxide is endothermic, requiring 99.5 KJ/mol of energy (da Costa et al., 2013). The reduction steps are presented in the Eqs. (3), (4) and (5).

$$3Fe_2O3(s) + H_2(g) \rightarrow 2Fe_3O_4(s) + H_2O(g) \quad (3)$$

$$Fe_3O_4(s) + H_2(g) \rightarrow 3FeO(s) + H_2O(g) \quad (4)$$

$$FeO(s) + H_2(g) \rightarrow Fe(s) + H_2O(g) \quad (5)$$

Hydrogen can be combusted in the DRI shaft furnace to provide the thermal energy required for the endothermic reaction (Duarte and Pauluzzi, 2019). This would require input of higher flow rate of hydrogen than the stoichiometric requirement. For this analysis, a flow rate 10% excess hydrogen has been considered. However, the exact flow rate would depend on the process kinetics, thermodynamics, iron ore characteristics (diffusivity), heat transfer rate from the reactor walls etc, which is outside the scope of this analysis. The unreacted hydrogen can be fed back to the reactor, as has been depicted through the stream **Residual H_2**. Metallization rate of 94% is achieved in the SF. Metallization rate refers to the ratio of metallic iron entering and leaving the shaft furnace. The metallic stream (mixture of Fe, FeO and impurities) exits the shaft furnace at a temperature of 700 °C. It is depicted by **M2** in the figure. Unreacted hydrogen and water leave the SF at a temperature of 300 °C from the shaft furnace through the stream **M5**.

2.2.2. Hot metal transport

The metallic stream, **M2**, can be either cooled down to form cold direct reduced iron (CDRI) or can be fed to a briquetting machine to form hot briquetted iron (HBI). The CDRI and HBI can be shipped to other locations where they can be fed to an EAF or BF for steel production. However, in this analysis, the hot iron feed at 700 °C is directly fed into the EAF. This reduces the energy consumption of the EAF. Since the energy consumption of DRI with zero carbon is higher than in the EAF, it is beneficial to take advantage of the hot metal stream and produce molten steel in the integrated process. Feeding the burden at 700 °C results in an energy saving of approximately 140 KWh/tls. An additional advantage is the extended lifetime of graphite electrodes, and refractory layer of the EAF. The largest DRI-SF reactor manufacturers, ENERGIRON and MIDREX offer solutions for the transport of hot metal from the SF to the EAF. Energiron's HYTEMP™ system uses a pneumatic transport system (Energiron, 2022). The HOTLINK™ system designed by MIDREX on the other hand uses gravitational forces for the transfer of the burden from the SF to the EAF (Midrex, 2021).

2.2.3. Electric arc furnace

The incoming metallic stream is heated to a temperature of 1650 °C inside the EAF. The EAF operates with a charge of 100% hot DRI from the SF. Carbon fines, **M6**, are added to the EAF to reduce the FeO, and for the production of CO, which is essential for froth formation, and slag removal inside the EAF. Froth formation extends the life of the refractory lining, graphite electrodes and reduces downtime of the EAF (Kirschen et al., 2011). Slag is removed from the EAF by using slag formers(CaO, MgO). The slag stream,**M8**, leaves the EAF at a temperature of 1650 °C. Oxygen produced as a by-product of the electrolysis, finds application in the EAF, where it helps in the oxidation of carbon fines to CO. The oxidation reaction is exothermic, and contributes in reducing the overall electricity consumption of the EAF. Air enters the EAF during opening and closing of the roof for material input. Combination of CO_2, NO_2, NO leave the EAF as exhaust gases through **M9** at a temperature of 1500 °C. Energy from the exhaust stream could be used to heat the SF or the hydrogen stream, but this process integration has not been considered in this analysis. The molten metal stream, **M3**, leaves the EAF at a temperature of 1650 °C. The molten metal could either be converted to billets for export or processed further. Subsequent processing of the steel would require additional capital investment and energy inputs. This has not been considered in the present analysis.

2.2.4. Hydrogen production

Alkaline electrolyzers are the most advanced electrolyzers systems, have been deployed at industrial scale previously, and are available in MW scale module sizes at present. Their costs are significantly lower than the other electrolyzer technologies such as polymer electrolyte membrane(PEM), and solid oxide electrolyzers, and their large-scale production is not constrained by availability of rare-earth materials like Platinum or Iridium (used for PEM electrolyzers) (David et al., 2019). A 4.5 MW Alkaline electrolyzer system, supplied by Nel Hydrogen, is being used to produce hydrogen for the H_2-SF demonstration plant commissioned in Sweden in August, 2020 (Pei et al., 2020). Alkaline electrolyzer have been considered for hydrogen production in this analysis.

The technical specifications of multi-MW scale alkaline electrolyzer modules available in the market is presented in Table 1. The average stack-life time of 80,000–100,000 h, and system life of 20–25 years has

Table 1
Technical specification of Alkaline electrolyzer systems available in the market.

Company	Units	Nel Hydrogen	thyssenkrupp	Sunfire	Tianjin Mainland Hydrogen Equipment
Electrolyzer model		A4000	20 MW module	HYLINK Alkaline	FDQ800
Net production rate	Nm^3/h	2400–3800	4000	2230	400–1000
Production capacity dynamic range	%	15–100	10–100	20–100	40–100
Power rating	MW		20	10	N.A
Power consumption at stack	KWh/Nm^3	3.8 to 4.4	4.5	N.A	4.4
Power consumption system level	KWh/Nm^3	N.A	N.A	4.7	N.A
System electrical efficiency(LHV)	%	N.A	N.A	64	N.A
Purity	%	99.99	99.99	99.99	99.99
Delivery pressure	Bar(gauge)	1 to 200	0.5	30	30
Electrolyte		25% KOH	N.A	N.A	30% KOH
Feedwater consumption	L/Nm^3	1	<1	1.9	N.A
Reference		nelhydrogen (2022)	thyssenkrupp (2022)	sunfire (2022)	TianjinMainlandHydrogenEquipment (2022)

been widely reported in the academic and gray literature (Matute et al., 2019). The reported system efficiency is in the range of 60%–67%, but can improve to 75%–80% in the future, based on improvements in the design of different electrolyzer components (IRENA, 2020). The electrolyzer system comprises of the electrolyzer stack, balance of plant systems like the gas separators, compressors(if required), electricity conversion devices (transformers and rectifiers), hydrogen purification system, water supply purification system, cooling equipment etc. High pressure compressors could be required on the storage loop. The reported cost of alkaline electrolyzer system including the balance of plant costs are in the range of $500–1000/$kW_{el}$ (IRENA, 2020). The costs of engineering, shipping the equipment, civil works and site preparations are additional to these costs. With the combined effects of technology learning, standardization of manufacturing components, automation of production processes, and improvements in performance parameters (lifetime, efficiency and durability), the capital costs of the electrolyzer systems could reduce substantially. Vartiainen et al. have projected the electrolyzer system cost to decline with a learning rate of 18% annually, and reach a capital cost of approximately $275/$kW_{el}$ by 2030 (Vartiainen et al., 2021). Standardization and technology learning from the Chlor-alkali industry could be directly applicable to the water–electrolyzer industry. Some of the largest chlor-alkali salt–electrolyzer manufacturers like thyssenkrupp uhde chlorine engineers, Asahi Kasie, De Nora etc. are venturing into the water electrolysis business.

Hydrogen stream exiting the electrolyzer, **M10** is pre-heated in the recuperator, by exchanging heat with the SF exhaust stream. The pre-heated H_2 stream, **M11** is heated to the reactor inlet temperature of 800 °C in the electrical heater. The SF exhaust stream, exit the recuperator at a temperature of 120 °C to ensure no condensation inside the heat exchanger tubes, through the stream **M12**. Excess H_2 dissolved in the exhaust stream is separated in the condenser and is fed back to the heater. Electrical gas heaters have been considered in this analysis, however it is possible to use hydrogen as a fuel. A final decision regarding the selection of the heaters would depend on both the capex and efficiency of gas heaters. Fossil fuel fired gas heaters are used in the industry quite frequently but would lead to the release of emissions, and have thus not been considered in this analysis. Water stream exiting the condenser at 70 °C, as **M13** can be fed back to the electrolyzer. Oxygen is produced as a by-product in the electrolyzers, and the exits the electrolyzer as **M14**. Part of it is used within the EAF and the remaining can be sold in market to generate additional revenue. In Norway, fish farms have high demand for Oxygen, and deploying a supply chain for the same could be beneficial for the overall plant economics. Purified water stream enters the electrolyzer for the production of Hydrogen.

2.2.5. Hydrogen storage

Hydrogen produced from the electrolyzer can be directly fed to the DRI shaft reactor or stored in the hydrogen storage unit. Hydrogen storage systems can be divided into two broad categories i.e. physical storage and chemical-based storage. Physical storage of H_2 refers to storing it under high pressure (60–960 Bar) or cryogenic storage of hydrogen at −253 C. Until now physical storage of hydrogen is the most widely deployed mode for commercial storage of hydrogen. Chemical-based storage systems, such as metal hydrides (AlH_3, MgH_2), ammonia, methanol, formic acid, or liquid organic hydrogen carriers are still at an early stage of development. Most of them require conversion and re-conversion processes, which require additional capital investment, and would lead to additional operational costs. Liquefaction of hydrogen at −253 °C, increases the volumetric energy density of H_2 significantly, but is an energy intensive process, requiring close to 10 KWh/kgH2 or one-third of the energy content of the hydrogen. Issues related to boil-off gases result in complicated insulation design requirements for the liquid H_2 storage tanks. In this analysis, compressed hydrogen storage has been considered as a viable alternative for storing hydrogen.

Compressed hydrogen can be stored in above-ground steel tanks or in underground geological reservoirs like salt and rock caverns, aquifers, or depleted oil and gas wells. Salt caverns are most suited for hydrogen storage and have been used in Texas (USA) since 1983 and in Teesside (UK) since 1972 (Abdin et al., 2021). Dilara et al. studied the technical potential of hydrogen storage in salt caverns in Europe (Gulcin et al., 2020). They estimated the total onshore and off-shore H_2 storage potential to be 84.8 PWh_{H_2}. Equinor and SSE thermal are building a salt cavern based hydrogen storage facility With an initial expected capacity of at least 320 GWh at Aldbrough. The storage plant is likely to be commissioned by 2028, and will comprise of nine salt caverns (Equinor, 2021). Under the HYBRIT project in Sweden, a lined rock cavern is being developed for hydrogen storage (Pei et al., 2020). Ahluwalia et al. calculated the levellized cost of hydrogen storage for underground pipe storage, salt caverns and lined rocks caverns. They found that storage in caverns gets cheaper as the storage capacity increases (Papadias and Ahluwalia, 2021). For a more detailed analysis on the levellized cost of storage, the readers are referred to the work of (Lord et al., 2014). While the cost of hydrogen storage in geological reservoirs is quite low, and reduces with increase in storage capacity, their availability is constrained by geographical formations.

Iberdola, which is building a 800 MW electrolyzer plant for green ammonia production in Puertollano, Spain will use steel tanks for Hydrogen storage (Iberdola, 2022). Each tank has a volume of 133 m^3, height of 23 meters and a diameter of 2.8 m, and can store 2.7 ton of hydrogen at a pressure of 60 Bar. Eleven such tanks will be installed at the plant. In order to meet the storage requirements of the proposed system, above-surface storage tanks made of austenitic stainless steels or aluminum have been considered in this analysis (Elberry et al., 2021). A capital cost of 1500 USD/kgH_2 has been considered for the system comprising of the compressors and storage tank (DEA, 2020). The operating pressure of the storage tank is considered to be 200 Bar. Transport of hydrogen within the plant can be done through the pipes made from L415ME/X60 grade steel, which is designed for oil and other combustible liquids, natural gas and other gaseous media. Arcelor Mittal is supplying pipes with similar grade of steel for a 440 kilometer, high-pressure hydrogen pipeline network across Italy, which could operate with 100% hydrogen (ArcelorMittal, 2022). Although the low-pressure pipes within the plant (except the storage lines) could be constructed with cheaper grades of steel.

Table 2
Capital cost assumptions.

Capital cost assumptions			
Equipment	Cost($)	Unit	Reference
Electrolyzer	$/kW	700	Vartiainen et al. (2021)
Stack replacement cost	$/kW	300	Vartiainen et al. (2021)
Shaft furnace	$t/steel/year	250	Krüger et al. (2020)
Electric arc furnace	$t/steel/year	160	Vogl et al. (2018)
Hydrogen storage tank	$kg/$H_2$	500	Hampp et al. (2021)
Hydrogen compressor	$kg/$H_2$	2545	Christensen (2020)

Table 3
Operational cost assumptions.

Operational cost assumptions			
Item	Cost	Unit	Reference/remark
Iron ore	120	$/t	OECD (2020)
Electrolyzer effciency(2020)	53	KWh/kgH_2	David et al. (2019)
Electrolyzer efficiency(2030)	45	KWh/kgH_2	David et al. (2019)
DRI OPEX	12	$/tls	Cavaliere (2019)
EAF OPEX	33	$/tls	Cavaliere (2019)
Emission price	100	$/t$CO_2$	EC (2020)
Grid emission factor(Norway)	16	gCO_2/KWh	EC (2020)

2.3. Economic evaluation

A discounted cash flow analysis was conducted to calculate the levellized cost of production for the proposed system. The levellized cost of production (LCOP) was calculated using Eqs. (6) and (7).

$$LCOP = \frac{C_{capex} * ACC + C_{opex} + C_{maint} + C_{labor} + C_{emission}}{Annual\ steel\ production} \quad (6)$$

Where, LCOP is the levelized cost of production, C_{capex} and ACC are the total capital investments, and annuity factor respectively. Annual operational, maintenance, labor and emission costs are represented by C_{opex}, C_{maint}, C_{labor} and $C_{emission}$ respectively.

$$ACC = \frac{r * (1+r)^n}{(1+r)^n - 1} \quad (7)$$

Where, r represents the discount rate used for the calculation and n refers to the plant life. A discount rate of 10% was considered in the base case to account for investments in an early stage technology. Plant life of 20 years, which is widely reported in the literature was considered for the calculations (Pimm et al., 2021).

The CO_2 mitigation cost was calculated for the different configurations, compared to the BF-BOF process using Eq. (8).

$$M_{cost} = \frac{LCOP_{SF-EAF} - LCOP_{BF-BOF}}{E_{BF-BOF} - E_{SF-EAF}} \quad (8)$$

In Eq. (8), M_{cost} is the mitigation calculated in $/tCO2. The numerator represents the difference in LCOP of the SF-EAF and BF-BOF system of similar capacity. The LCOP of the SF-EAF system is calculated using Eq. (6). For the BF-BOF system the LCOP has been varied between 400–500 $/t, based on widely reported literature values (Levi et al., 2022). E_{SF-EAF}, represents the sum of direct and indirect emissions from the SF-EAF system, and is calculated in tCO_2/tls. For the BF-BOF system, E_{BF-BOF}, represents the total emissions. A value of 2.1 tCO_2/tls has been used in this calculation (Backes et al., 2021).

2.3.1. Capital costs

The capital costs for the main plant components were calculated for a one Mtpa steel production plant, based on the material and energy balance from the conceptual process model. Equipment costs were converted to total capital costs using the Lang factors approach described by Sinnott et al. (Towler, 2013). A Lang factor of two was considered for the entire system. The electrolyzer installed capacity was calculated based on the flow rate of hydrogen, and corresponding efficiency. It was assumed that only the stacks, which are 60% of the electrolyzer system cost would be replaced after 90,000 h of operation. Compressor size was calculated based on the ideal gas equation, and outlet pressure of 200 Bar (Christensen, 2020). Capital cost assumptions for the main equipment are presented in Table 2.

2.3.2. Operational costs

To calculate the operational costs, price of iron ore, electricity, emission, and shaft furnace and EAF operational costs were considered. The electricity costs were determined using the optimization framework described in Section 2.3.3. Direct emissions from the plant were used to evaluate the annual emissions cost. The annual maintenance cost was considered to be 1.5% of the capital cost, and a labor cost of 20$/tls was allocated (Towler, 2013). Assumptions for evaluating the operational costs are presented in Table 3. It is assumed that the SF consumes 80 KWh/tls for the operation of the pneumatic system for the transport of iron ore from the hopper, operation of valves and transport of hot metal from SF to the EAF.

2.3.3. Electricity price

In this article, two scenarios for electricity procurement have been considered. In the first scenario electricity is procured based on long-term power purchase agreements. A fixed price of $60/MWh of electricity has been considered in the fixed electricity price scenario. For the second scenario, historical day-ahead prices for Bergen were retrieved from Nordpool (2020). Electricity prices are available at an hourly resolution for the different bidding zones in the Nordic electricity markets, including Oslo, Kristiansand, Bergen, Molde, Trondheim, and Tromsø. Bergen was chosen for the present analysis as it has the largest maritime port in Norway, handling more than 36% of the total cargo. As most of the iron ore will be imported, and the finished products would be shipped to EU countries, access to shipping routes could play a pivotal role in site selection. Historical day-ahead electricity prices were used to develop an optimal production schedule for the electrolyzers. Storage sizes were calculated based on the electrolyzer operation profile. Five different electrolyzer configurations were evaluated in this work. In the base case, the output of the electrolyzer system was considered to be equal to the hydrogen demand from the steel plant. The hydrogen output capacity was increased to two times the hourly hydrogen demand in the highest configuration to evaluate the impact of increasing the electrolyzer size on the financial feasibility of the plant.

Optimization framework:. The operation scheduling of the electrolyzers has been formulated as a linear optimization problem, shown in Eq. (9). Linear optimization formulation was chosen to avoid computational complexity. Other approaches such as mixed integer linear programming, quadratic programming, stochastic decision making using Markov chain method have been used by other researchers for a more detailed analysis optimal control strategies. As the focus of this study is to present an initial assessment, linear optimization was found to be an adequate solution. Scheduling of grid connected electrolyzers have been solved using linear optimization models previously (Nguyen et al., 2019).

$$\begin{aligned} \text{Minimize} \quad & c_1 x_1 + \ldots + c_n x_n \\ \text{subject to} \quad & a_{11} x_1 + \ldots + a_{1n} x_n \geq b_1 \\ & \vdots \\ & a_{m1} x_1 + \ldots + a_{mn} x_n \geq b_m \end{aligned} \quad (9)$$

The objective of the optimization framework is to minimize the operating cost by utilizing the fluctuations in electricity prices. Electricity price is the cost vector c_i, which varies each hour, based on the historical day ahead prices. At each hour, a decision has to be made regarding the amount of hydrogen to be produced, which is represented

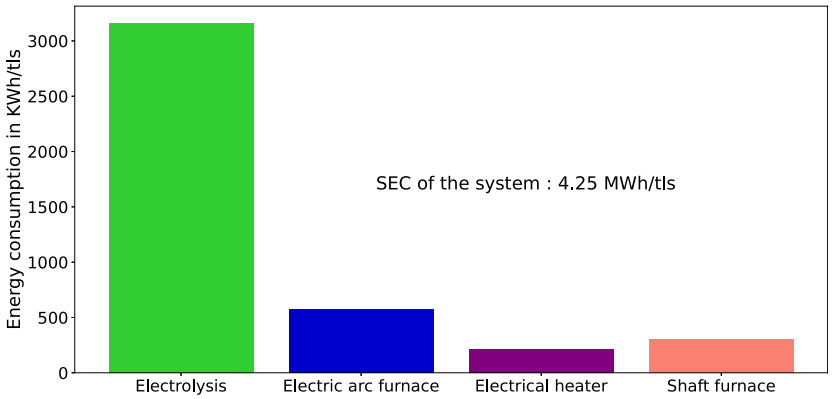

Fig. 2. Electricity consumption of different components of the H_2-SF-EAF system.

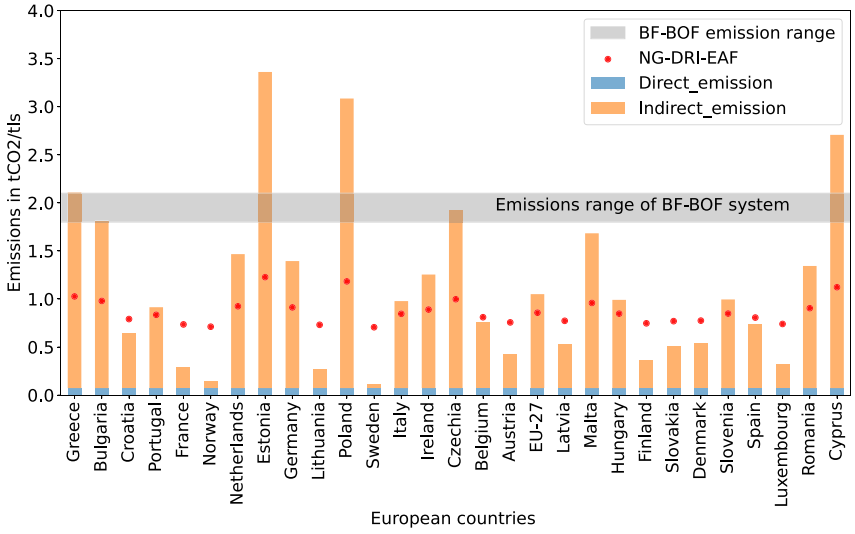

Fig. 3. Emissions from the hydrogen SF-EAF system in European countries.

Table 4
Lower and upper bounds of input variables for sensitivity analysis.

Input Variable	Units	Lower Bound	Upper Bound
Discount rate	%	0.06	0.12
Plant life	Years	20	40
Lang factor	Number	1	2
Electrolyzer efficiency 2020[a]	KWh/kgH2	60	45
Electrolyzer efficiency 2030[a]	KWh/kgH2	50	40
Electrolyzer capex 2020	USD/kW	600	800
Electrolyzer capex 2030	USD/kW	300	500
EAF capex	USD/t/Year	100	200
DRI-SF capex	USD/t/Year	200	300
Iron ore cost	USD/t	80	150
Electricity price[b]	USD/MWh	40	100
Grid emission factor	tCO2/KWh	0.015	0.250
Emission price	USD/tCO2	50	250
Storage unit cost[c]	USD/kGH2	100	500

[a]In the model, the lower bound has to be numerically lower.
[b]Electricity price was varied for configuration with fixed power prices.
[c]Storage input costs were varied only for the configuratons purchasing electricity from the day-ahead market.

by the decision variable x_i. The optimization is done for every twenty four hours, since day-ahead prices are available for the next 24 h. In order to get the annual hydrogen generation profile, the slice of the cost vector is passed to the optimization function, which generates an instance of the optimization problem for every 24 h. To calculate the annual operational cost the code is run 365 times, as the optimization interval is fixed at 24 h. The analysis was conducted for all five electrolyzer configurations. The quantity of hydrogen produced per hour is constrained by the installed electrolyzer capacity, defined in Eq. (10).

$$0 \leq x_i \leq \text{electrolyzer capacity} \tag{10}$$

The second constraint pertains to the meeting the demand of hydrogen. At each hour, the demand for hydrogen, represented by b_i has to be met. Hydrogen could be supplied by the electrolyzer or through the hydrogen storage unit. Considering the fixed demand of hydrogen for steel making to be d tons/hour, the demand vector is presented in Eq. (11):

$$b_j = \sum_{n=1}^{24} d * n; \text{where j varies from 1 to 24} \tag{11}$$

The generation profile was used to evaluate the storage status by transferring all excess hydrogen generated to the storage unit. Energy consumption of 0.4 MWh/t of hydrogen has been used for the compression process (Penev et al., 2019). The storage status at each instance can be calculated using Eq. (12)

$$s_k = \sum_{n=1}^{k} x_k - d_k; \tag{12}$$

Where $s = 0, t = 0$, k is the hour, which varies from 1 to 8760.

Table 5
Material and Energy flows through the system.

Stream	Stream description	Material flow (kg/tls)	Temperature (°C)	Enthalpy (KWh/tls)
M1	Raw iron ore input	1504.99	25	0.0
M2	Metallic stream at SF outlet	1075.25	700	116.38
M3	Molten metal at EAF outlet	1000.0	1650	324.85
M4	Hydrogen stream at SF inlet	59.56	900	213.08
M5	SF exhaust stream	484.49	300	71.72
M6	Carbon fines added to EAF	20.0	25	0.0
M7	Slag formers added to EAF	75.0	25	0.0
M8	EAF exhaust gas stream	150.0	1500	89.09
M9	EAF slag stream	200.0	1650	49.29
M10	Hydrogen at electrolyzer outlet	59.56	70	1.12
M11	Hydrogen stream at electric heater inlet	59.56	170	29.54
M12	SF exhaust at recuperator outlet	484.49	120	24.13
M13	Water stream at condenser outlet	483.89	70	86.29
M14	Oxygen stream at electrolyzer outlet	476.49	25	0.0

2.4. Uncertainty analysis

The global sensitivity analysis was carried out using the SALib library to evaluate the Sobol first-order and Sobol total-order sensitivity indices (Herman and Usher, 2017). The parameters used for calculating the levellized cost of production were varied between the lower and upper bounds. Uncertainty propagation was calculated by varying the value of the input variables between the lower and upper bounds, and determining the relationship between the input variables and output variable, as well as the inter-dependence of the input variables. To get convergence the model was run 16384 times. The lower and upper bounds of the input parameters are presented in the Table 4.

3. Results

3.1. Material and energy flows

The material and energy flows through the different components of the system are presented in the Table 5.

3.2. Energy consumption

The H_2-SF-EAF system has a specific energy consumption (SEC) of 4.25 MWh/tls, at an electrolyzer efficiency of 53 KWh/kgH_2. In the literature, the SEC of comparable systems vary from 3.48 MWh/tls (Vogl et al., 2018) to 3.95 MWH/tls (Krüger et al., 2020). The difference in the SEC's originate from the use of different electrolyzer types, values of electrolyzer efficiency (depends on the projected installation year of the plant), use of scrap in the EAF, thermal energy requirements of the shaft-furnace, purge-gas requirements etc. Water electrolysis was found to consume 75.7% of the total energy. Consumption of electricity from different components of the system is presented in Fig. 2.

3.3. Emissions

The total emissions from the system could be divided into direct and indirect emissions. Direct emissions from the EAF (lime production, carbon oxidation, FeO)reduction account for 73 kgCO_2/tls. Indirect emissions from pellet production, and lime production contribute to 167 kgCO_2/tls. While the upstream emissions do not vary substantially with location, the indirect emissions from electricity consumption vary with the electricity mix of the region where the plant is located. The indirect emissions from electricity consumption were found to be 67 kgCO_2/tls. A comparison of the total emissions from the H_2-SF-EAF operation in different countries is shown in Fig. 3. The red dots represent the average emissions from a natural gas based DRI-EAF plant, whereas the gray band represents the emission range of the BF-BOF process. It can be inferred from this chart that countries with low grid emission factor like Norway and Sweden are well suited for the installation of H_2-SF-EAF plants, in terms of total emission reduction.

3.4. Hydrogen production and storage status

The H_2-SF-EAF plant was found to have an hourly hydrogen demand of 7.55 tons/h. The hourly demand is met either through production or from hydrogen produced earlier and stored in the storage tanks. In Fig. 4, histogram of the hydrogen production and storage status for different configurations is presented. The configuration with constant production, and no storage have been excluded from the plot for brevity. Hydrogen production profile have been presented on the left and the associated storage status at each hour is on the right hand of the chart. It can be observed from that the number of idle hours increase, as the capacity increases. By increasing the installed hydrogen output capacity from 7.55 t/h to 15.11 t/h, electricity demand could be shifted for more than 43% of the time. Shifting industrial electricity demand, often referred to as demand response, has the potential to increase the flexibility of the grid, and allow integration of intermittent renewable electricity generators (Stöckl et al., 2021). Hydrogen storage tanks remain empty for shorter duration, only 16% of the time for configurations with higher hydrogen output. To double the hydrogen production capacity from 7.55 t/h to 15.11 t/h, hydrogen storage tanks with a capacity of 90 tons would be required.

3.5. Levelized cost of steel production

LCOP of $714/t was calculated for the configuration with fixed electricity price of $60/MWh. For the systems procuring electricity from the day-ahead markets, the LCOP varied from $622-$722/t. The LCOP values, for all configurations, were found to be significantly higher than the LCOP of the plants based on BF-BOF process. LCOP of the different configurations is shown in Fig. 5. The configurations are shown on the *x*-axis, according to their hydrogen output capacity. The right most column(7.55-ppa) represents the configuration with a hydrogen out put capacity of 7.55 t/h, while purchasing electricity at under a fixed power purchase agreement. Almost 73% of the LCOP is comprised of the operational cost, which is primarily composed of the electricity costs and iron ore costs. While the operational costs have the maximum contribution to the production costs at lower hydrogen output capacities, the contributions from capex become more prominent for the configurations with higher electrolyzer capacities. The maintenance costs increase with higher capacities, while the labor and emission costs remain constant for all configurations at $20 million and $7.64 million respectively. The emission costs were calculated only for the direct emissions from the H_2-SF-EAF system.

Capital cost. The capital cost of the system configurations with higher hydrogen flow rates were found to be significantly higher, owing to the need for larger installed capacity of electrolyzer, storage tanks and compressor systems. It was found that doubling the electrolyzer capacity, and subsequent shifting of operating hours, would require 90 tons of storage capacity, and a compressor of 13.6 MW electrical capacity

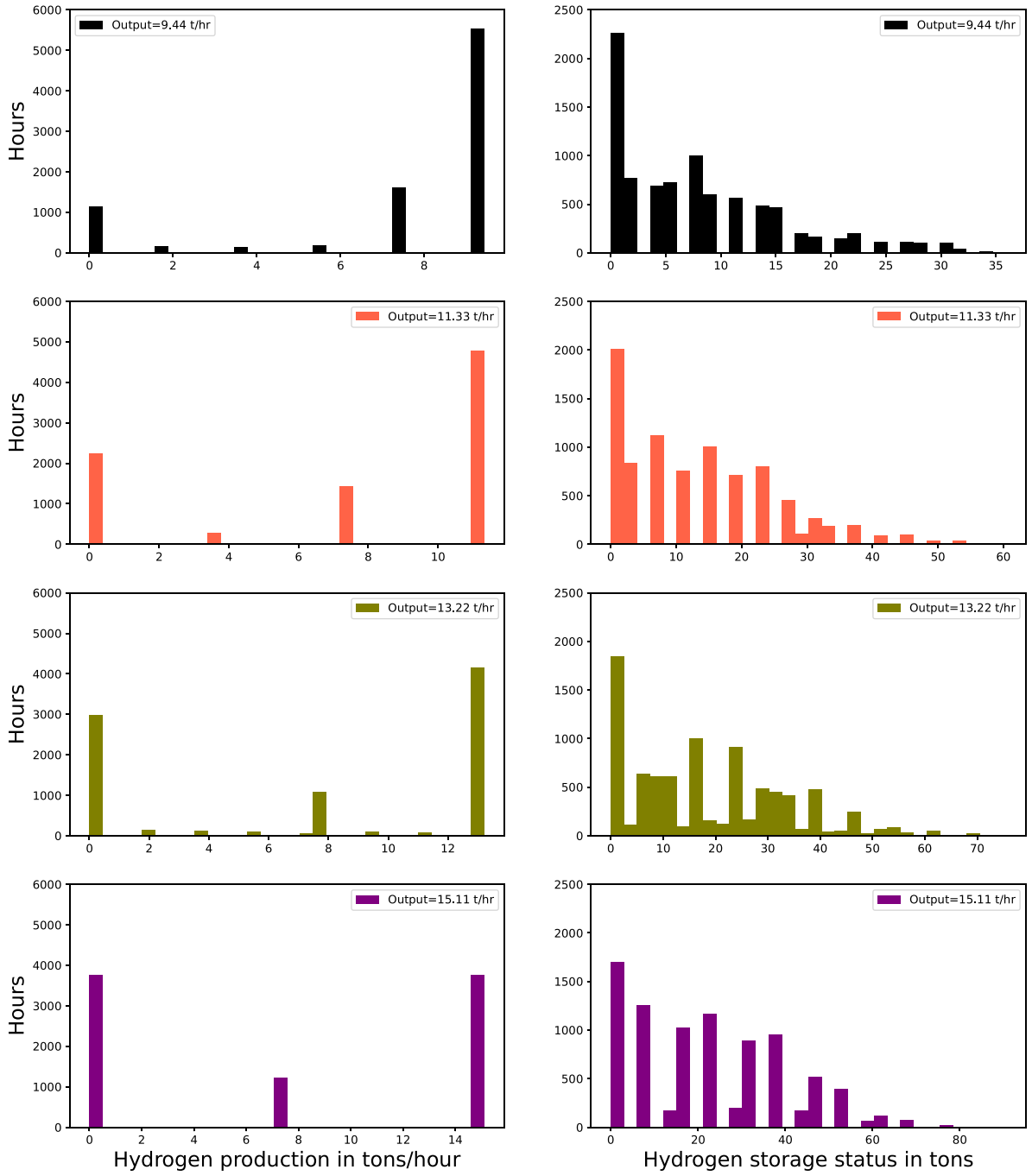

Fig. 4. Histograms of production and storage status of different electrolyzer configurations.

Table 6
Capital cost distribution of different plant configurations.

Configurations	Electrolyzer	Stack replacement	DRI-EAF capex	Storage capex	Compressor capex
7.55	280.10	61.15	410,00	0,00	0,00
9.44	350.22	76.46	410,00	17.95	9.57
11.33	420.34	91.77	410,00	30.02	19.1
13.22	490.46	107.08	410,00	37.75	28.71
15.11	560.581	122.39	410,00	45.3	38.28
7.55 _PPA	280.10	61.15	410,00	0,00	0,00

*All costs are in Million USD.

to deliver the required flow rate. The distribution of capital costs for the six different configurations analyzed in this work is presented in Table 6.

Electricity cost. The electricity costs where found to be highest for the configuration purchasing electricity at a fixed electricity price. Purchasing electricity from the day-ahead market could reduce the procurement cost of electricity by 38%, if the electrolyzer capacity

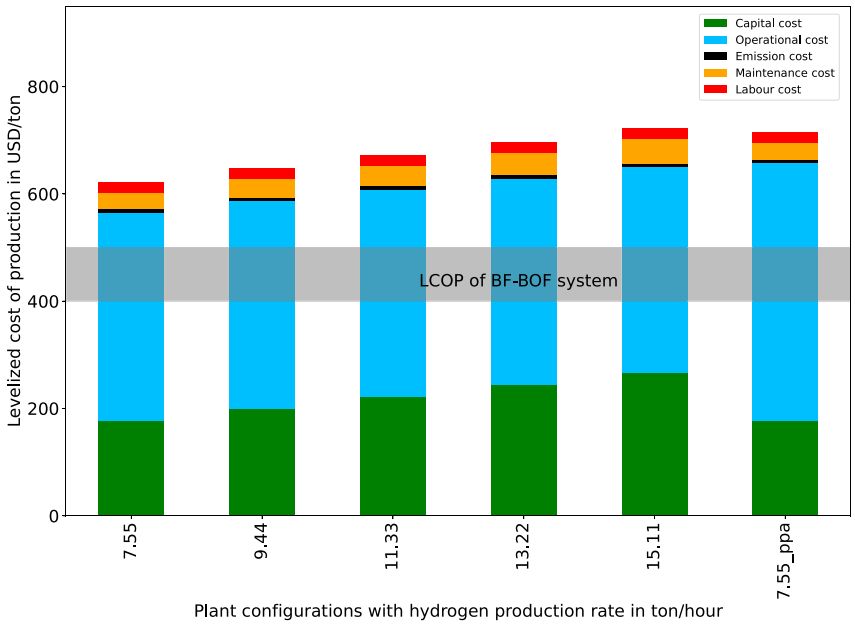

Fig. 5. Levelized cost of production for different plant configurations.

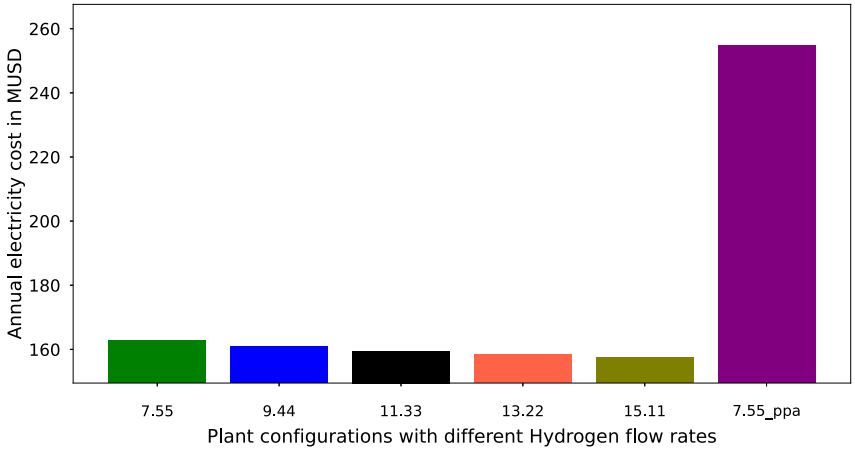

Fig. 6. Annual electricity costs for different configurations.

is doubled, and storage tanks are installed at the facility. However, even at the same electrolyzer capacity, procuring electricity from the markets instead of fixed power purchase agreements could bring down annual electricity costs from $254 million to $160 million. In Fig. 6 for the different configurations is presented.

3.6. Sensitivity analysis

The results of the global sensitivity analysis in the form of first order Sobol indices, and total order Sobol indices are presented in this section. The values of the second order Sobol indices were found to be insignificant, indicating weak interaction between the input variables, and hence have not been included in this analysis.

3.6.1. Configuration with fixed PPA

For the system procuring electricity at fixed price, variation in the price of electricity could have the maximum impact on the LCOP. Iron ore price, Lang factor, and electrolyzer capex are the other important parameters. For configurations with lower electrolyzer capacity, iron ore prices have a higher contribution to the total uncertainty. The lower impact of the interest rate indicate that LCOP is heavily dependent on the operational costs (see Figs. 7 and 8).

3.6.2. Configurations purchasing electricity from day-ahead markets

Fluctuation in iron ore price affects the systems with lower hydrogen output capacity, and hence lower capital investments, while configurations with higher output of hydrogen show higher sensitivity to installation costs(Lang factor), and the interest rate (discount rate). Plant life also becomes a significant factor for the plants with increased capital investments, as it a part of the annuity calculations. Longer lifetime of plants could reduce the LCOP. Storage cost does not have a huge impact owing to the relatively smaller size.

4. Electricity price data characteristics

The current work focuses on developing an optimization model, based on linear optimization techniques for operational scheduling based on day ahead electricity prices. Further insights can be derived by understanding the seasonal variation in electricity prices which can aid in developing an optimal strategy for plant/storage sizing as well.

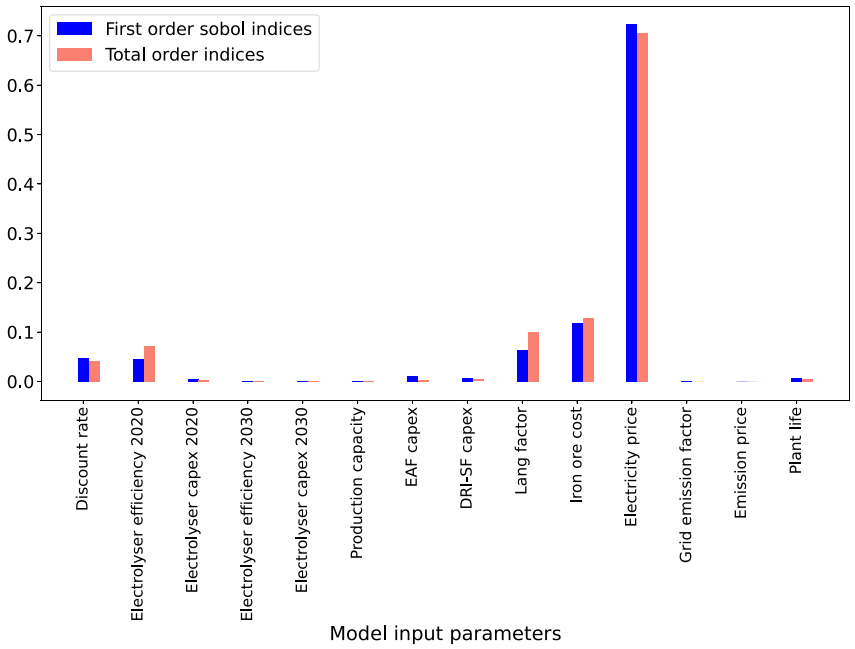

Fig. 7. Sensitivity analysis for the configuration purchasing electricity at fixed price.

The combination of high degree of variability in electricity demand and supply creates a regional price environment that may have daily, weekly, seasonal or yearly characteristics. This section provides a brief of the price characteristics in Bergen region of Norway for the year 2019 which has been used for the optimization performed in this study.

The electricity prices for the Bergen region in the year 2019 is shown in Fig. 9. Analyzing a time series like the electricity prices shown in Fig. 9 involves data mining to extract knowledge from the data. One of the methods to gain a deeper understanding of the data and extract patterns and anomalies embedded in the dataset, is Time Series sub-sequences All-Pairs-Similarity-Search (TSAPSS). Matrix profile is a innovative and fast technique for performing TSAPSS proposed by researchers at University of California, Riverside and University of New Mexico (Yeh et al., 2017) in 2016. Briefly, the Matrix profile of a time series of length n is itself a time series that contains the z-normalized Euclidean distance normalized distance of a sub-sequence of length m to its nearest neighbor in the original time series (Yeh et al., 2018). Annotating the original time series with the matrix profile can help locate the motifs (closely repeated patterns) and discords (anomalies). Further, the matrix profile allows us to perform semantic segmentation and identify the existence of regimes in a time series based on the calculation of a Corrected Arc Crossing (CAC) for every data point in the series (Gharghabi et al., 2017).

The matrix profile for the time series in this study was computed with a sub-sequence length of 1 week ($m = 24 * 7 = 168$ hours). Based on the matrix profile, the CAC and the locations of the regime change has been plotted in the lower half of Fig. 9. Fig. 9 shows that the major seasons (summer and winter) form a distinct price regime, while the shoulder seasons are split roughly in the middle indicating a transition period. A future work could investigate leveraging the existence of these seasonal regimes for calculating optimum storage sizing and exploring the possibility of incorporating large scale sub-surface storage. Large scale storage systems like salt caverns which are cycled seasonally enable continuous production of Hydrogen for extended periods. Additionally, this can be an effective strategy for de-risking against price fluctuations in the electricity market.

The motif and discords extracted form the price data are shown in Fig. 10. From the pattern matches obtained in Figs. 10(a) and 10(b) we can see that these weekly periods represent periods with very low daily fluctuation on prices with bi-modal peaks. The twice daily peaks can be attributed to morning and evening peak load periods, however, it is interesting to note that the dips between these periods remains relatively low. The third motif (Fig. 10(c)) has similar characteristics however, the peaks during the first two days are much higher. The black anomaly shown in Fig. 10(d) is interesting since there is no clear daily pattern in this period and very high variability. A future work could also explore the utilization of motifs (repeated patterns) and discords (anomalies) in the price data. The current analysis has been done for patterns of sub-sequence length: 1 week. Performing the analysis at varying sub-sequence lengths relevant to the operation of the plant could lead to significant insights. For instance identifying the nature of anomalous periods and linking them to prevailing regional and environmental conditions can help us predict these periods. As mentioned previously, over one-third of electricity generation in Norway is used for energy intensive industrial applications. Performing a similar analysis with electricity price data overlaid with wind/ solar energy generation potential on a regional basis can further aid the case for greater investments in renewable energy production to facilitate the development of decarbonized heavy industries in Norway.

5. Discussion

BF-BOF based steelmaking process has been optimized for several decades, and has an advantage over the H_2-SF-EAF process in terms of cost. However, in a carbon constrained world, the cost of operating a BF-BOF based steel mill could increase substantially. With increasing carbon taxes, as envisaged in the revised EU emission trading system, the LCOP of BF-BOF based could increase substantially. Increase in cost of raw materials such as coking coal has increased the production costs considerably for steel producers in recent times (Levi et al., 2022). Reduction in electrolyzer capex, efficiency improvements, and reduced cost of finance could bring down production costs for H_2-SF-EAF based steel based route The emission price at which an alternatively technology could become economically feasible is often used as a metric to evaluate different decarbonizing technologies. The CO_2 mitigation cost range for the different configurations is presented in Fig. 11. The mitigation costs were found to vary from \$68/tCO_2 to \$180/tCO_2. The emission trading price in the EU has increased from \$40/tCO_2 to \$90/tCO_2 in the past year, and the increasing trend is likely to continue in the coming years, on the back of ambitious climate policies.

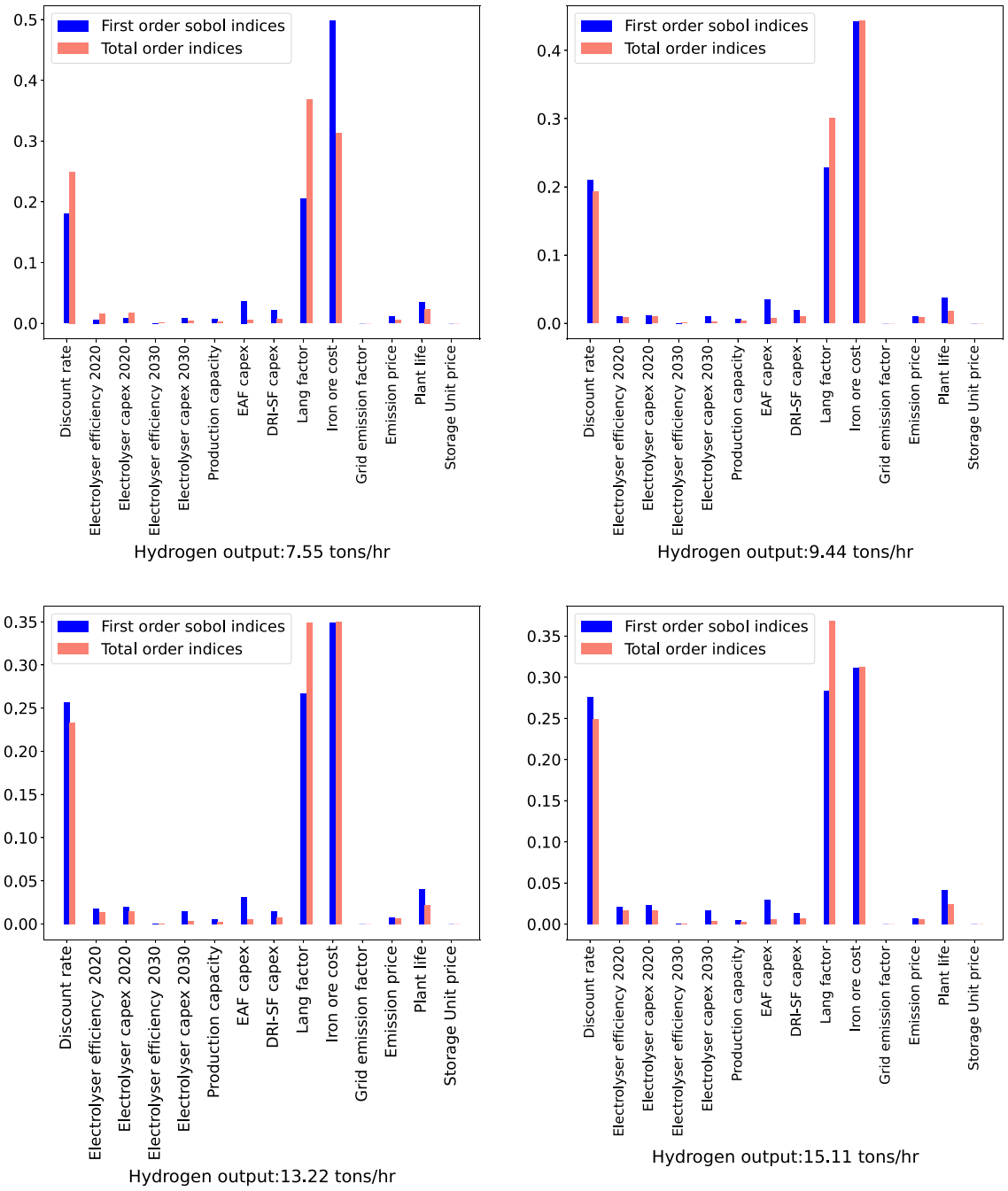

Fig. 8. Sensitivity analysis for the configuration purchasing electricity from the day-ahead electricity markets.

6. Conclusion

In this work, techno-economic assessment of a grid connected H_2-SF-EAF plant in Bergen, Norway was conducted to answer a set of research questions. An open-source model was developed to calculate the levelized cost of production for two configurations i.e. one purchasing electricity at a fixed price, and the other procuring electricity from the day-ahead electricity markets. The main findings, in light of the research questions are discussed below.

What are the enabling factors associated with the H_2-SF-EAF based steel production in Norway?. The main influencing factors identified in this analysis are availability of cheap and low-emission electricity, access to magnetite iron ore from northern Norway(Varanger), access to the EU market, and availability of a highly-skilled workforce. Some of the other factors, which could further add to the attractiveness of Norway as a hydrogen based steel manufacturing destination are its offshore wind energy potential, and a need for the economy to transition from the oil and gas industry.

What is the levellized cost of hydrogen based steel production in Norway?. The levellized cost of steel production varied from $ 622 to $722 for the different configurations. The production costs were found to be 40% higher than the BF-BOF based steel production route. CO_2 mitigation cost was found to vary between \$68/tCO_2 to \$180/tCO_2.

Which electricity procurement strategy; fixed power purchase agreements or procurement of electricity from day-ahead electricity markets is most cost-efficient?. Participating in the electricity markets could reduce production costs by 14,7% compared to a plant with similar capacity,

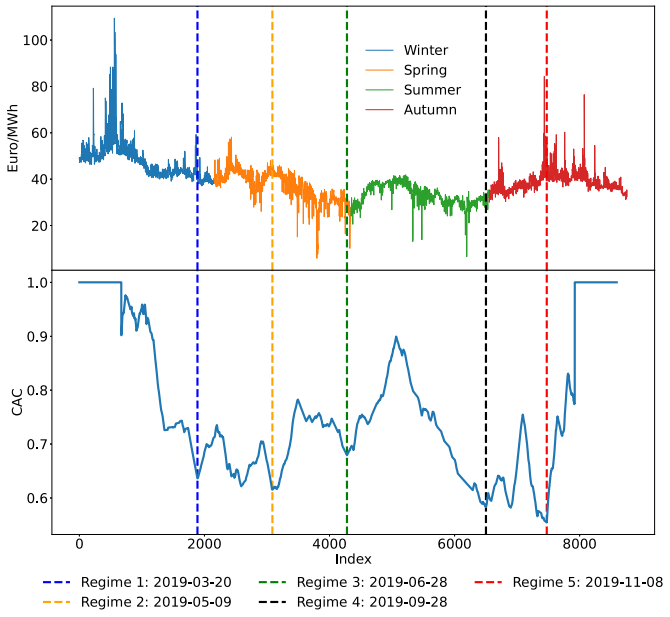

Fig. 9. Seasonal variation of electricity prices in Bergen (2019) and the regime changes based on the Corrected Arc Crossings (CAC).

operating with fixed electricity prices. Increasing the electrolyzer capacity reduced the operational costs. However, the reduction was not enough to justify investments in additional electrolyzer, and hydrogen storage capacity. Access to underground geological storage such as salt cavern, rock cavern or depleted oil wells could make it economically feasible to store large quantities of hydrogen at cheaper costs, and allow the plant to leverage the seasonal fluctuation in electricity costs. It would also open opportunity for the steel plant to participate in the electricity capacity markets and generate additional revenue. Analyzing the historical price trends could help in detection of seasonal patterns in electricity prices, which could be leveraged for designing a plant with optimal plant capacity and operation schedule.

Abbreviations

EU	European Union
USA	United States of America
UK	United kingdom
IDDI	Industrial deep decarbonization initiative1
DRI	Direct reduced iron
HBI	Hot briquetted iron
SF	Shaft furnace
HDRI	Hydrogen direct reduced iron
HYFOR	Hydrogen-based fine-ore reduction
NIST	National institute of standards
EAF	Electric arc furnace
BF-BOF	Blast furnace basic oxygen furnace
SMR	Steam methane reforming
CAC	Corrected Arc Crossings
LCOP	Levelized cost of production
IPCC	Inter-governmental panel on climate change
SSAB	Svenskt Stål AB
LKAB	Luossavaara-Kiirunavaara Aktiebolag
MMBTU	Metric Million British Thermal Unit
IDDI	Industrial deep decarbonization initiative
SEC	Specific energy consumption
tls	Ton of liquid steel
$kgCO_2$	Kilogram of carbon dioxide
tCO_2	Tonn of carbon dioxide
$GtCO_2$	Gigaton of carbon dioxide
kg	Kilogram
kJ	KiloJoule
GJ	GigaJoule
kW	kilowatt
kW_{el}	kilowatt electric
MW	Megawatt
GW	Gigawatt
KWh	Kilowatthour
MWh	Megawatthour
TWh	Terrawatthour
Mtpa	Million ton per annum
mol	moles
L	Liter
NM^3	Normal cubic meter
h	hour
CO	Carbon Monoxide
H_2	Hydrogen
O_2	Oxygen
Al_2O_3	Aluminum oxide (Alumina)
SiO_2	Silicon dioxide(Sillica)
Fe_2O_3	Hematite
Fe_3O_4	Magnetite
Fe	Iron
FeO	Iron Oxide
Fe_3C	Iron carbide
C	Carbon
CO_2	Carbon dioxide
NO_2	Nitrous Oxide
MgO	Magnesium Oxide
CaO	Calcium Oxide

Symbols

$	US Dollar
USD	US Dollar
°C	Celsius
€	Euro
$M1$	Iron ore stream entering the shaft furnace in kg/tls
$M2$	Metallic stream exiting the shaft furnace in kg/tls
$M3$	Molten steel exiting the electric arc furnace kg/tls
$M4$	Hydrogen stream entering the shaft furnace in kg/tls
$M5$	By-product Water and unreacted Hydrogen exiting the shaft furnace in kg/tls
$M6$	Carbon fines added to the electric arc furnace in kg/tls
$M7$	Slag formers added to the electric arc furnace in kg/tls
$M8$	Slag stream exiting the electric arc furnace in kg/tls
$M9$	By-product gases exiting the electric arc furnace in kg/tls
$M10$	Hydrogen stream exiting the electrolyzer in kg/tls
$M11$	Hydrogen stream exiting the recuperator in kg/tls
$M12$	By-product Water and unreacted Hydrogen exiting the recuperator in kg/tls
$M13$	Water stream exiting the condenser in kg/tls
$M14$	Oxygen stream exiting the electrolyzer in kg/tls
$H1$	Enthalpy of stream M1 in KWh/tls
$H2$	Enthalpy of stream M2 in KWh/tls
$H3$	Enthalpy of stream M3 in KWh/tls
$H4$	Enthalpy of stream M4 in KWh/tls
$H5$	Enthalpy of stream M5 in KWh/tls
$H6$	Enthalpy of stream M6 in KWh/tls
$H7$	Enthalpy of stream M7 in KWh/tls

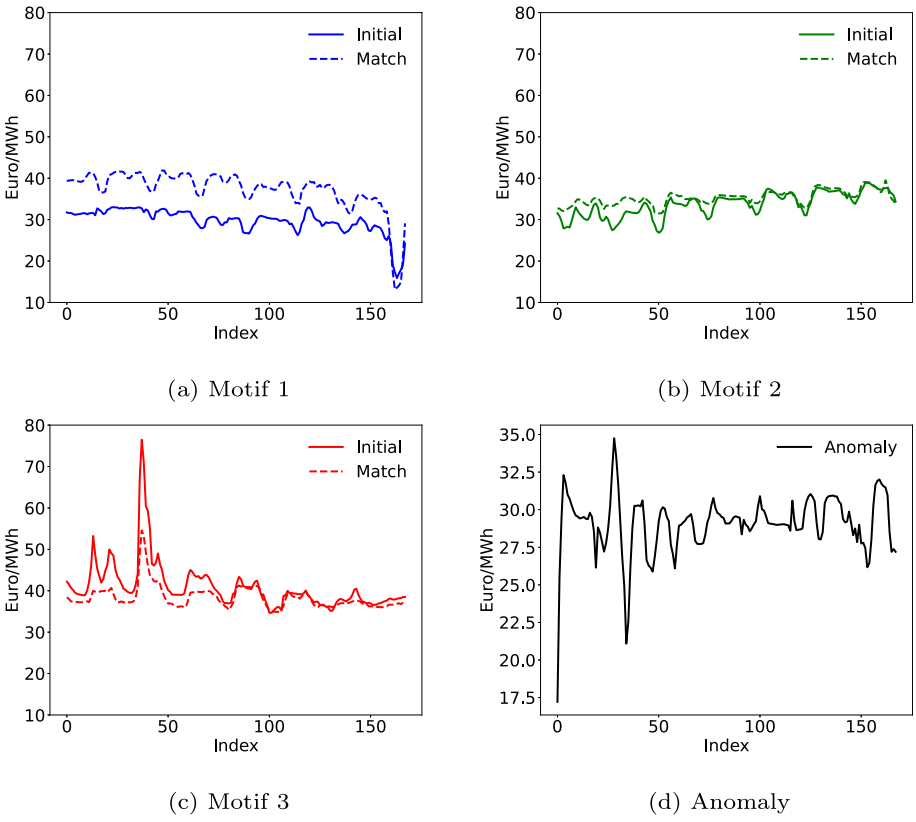

Fig. 10. Closely repeating patterns (a–c) of length 1 week and an anomalous (d) 1 week period with high variability detected in the 2019 Bergen day ahead electricity prices.

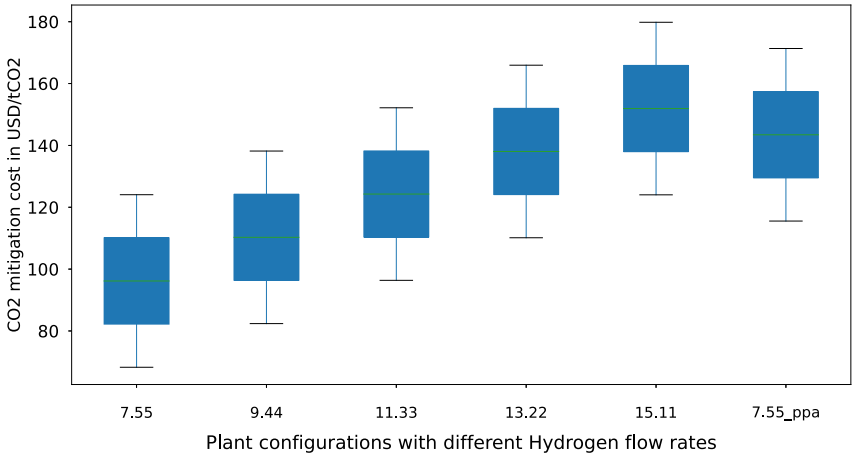

Fig. 11. CO_2 mitigation costs for different configurations.

$H8$	Enthalpy of stream M8 in KWh/tls
$H9$	Enthalpy of stream M9 in KWh/tls
$H10$	Enthalpy of stream M10 in KWh/tls
$H11$	Enthalpy of stream M11 in KWh/tls
$H12$	Enthalpy of stream M12 in KWh/tls
$H13$	Enthalpy of stream M13 in KWh/tls
$H14$	Enthalpy of stream M14 in KWh/tls

Funding

This project has received funding from the European Union's Horizon 2020 research and innovation programme under the Marie Skłodowska-Curie grant agreement No 765515.

CRediT authorship contribution statement

Abhinav Bhaskar: Conceptualization, Methodology, Software, Visualization, Investigation, Data curation, Writing – review & editing. **Rockey Abhishek:** Data curation, Writing – original draft, Investigation, Software, Visualization. **Mohsen Assadi:** Supervision, Funding. **Homam Nikpey Somehesaraei:** Supervision, Funding.

Declaration of competing interest

The authors declare that they have no known competing financial interests or personal relationships that could have appeared to influence the work reported in this paper.

Data availability

Python codes used for modeling the H_2 -SF-EAF system and calculating the optimal electrolyzer production schedule are available at Zenodo repository (Bhaskar, 2021).

Acknowledgments

The authors would like to thank Kevin Gould from Statkraft for his valuable inputs and advice. The authors appreciate the feedback and suggestions received from anonymous reviewers.

References

Åhman, M., Olsson, O., Vogl, V., Nyqvist, B., Maltais, A., Nilsson, L.J., Hallding, K., Skånberg, K., Nilsson, M., 2018. Hydrogen steelmaking for a low-carbon economy: A joint LU-SEI working paper for the HYBRIT project. p. 28, Stockholm environment institute and Lund University, Stockholm, URL: https://www.sei.org/wp-content/uploads/2018/09/hydrogen-steelmaking-for-a-low-carbon-economy.pdf.

Abdin, Z., Tang, C., Liu, Y., Catchpole, K., 2021. Large-scale stationary hydrogen storage via liquid organic hydrogen carriers. IScience 24, 102966. http://dx.doi.org/10.1016/j.isci.2021.102966.

Andersson, J., 2021. Application of liquid hydrogen carriers in hydrogen steelmaking. Energies 14, 1392. http://dx.doi.org/10.3390/en14051392, URL: https://www.mdpi.com/1996-1073/14/5/1392.

ArcelorMittal, 2022. Arcelormittal steels used in first hydrogen-certified pipeline.

Backes, J.G., Suer, J., Pauliks, N., Neugebauer, S., Traverso, M., 2021. Life cycle assessment of an integrated steel mill using primary manufacturing data: Actual environmental profile. Sustainability (Switzerland) 13, http://dx.doi.org/10.3390/su13063443.

Bailera, M., Lisbona, P., Peña, B., Romeo, L.M., 2021. A review on CO2 mitigation in the iron and steel industry through power to x processes. J. CO2 Util. 46, 101456. http://dx.doi.org/10.1016/j.jcou.2021.101456, URL: https://linkinghub.elsevier.com/retrieve/pii/S2212982021000238.

Bhaskar, A., 2021. Levellized cost of prodution of hydrogen based steel production in bergen Norway, using a cost optimization framework for optimal scheduling of hydrogen electrolyzers. http://dx.doi.org/10.5281/zenodo.5520046, Zenodo, Oslo.

Bhaskar, A., Assadi, M., Somehsaraei, H.N., 2021. Energy conversion and management : X can methane pyrolysis based hydrogen production lead to the decarbonisation of iron and steel industry ? Energy Convers. Manage.: X 10, 100079. http://dx.doi.org/10.1016/j.ecmx.2021.100079.

Birat, J.-P., 2020. Society, materials, and the environment: The case of steel. Metals 10, 331. http://dx.doi.org/10.3390/met10030331, URL: https://www.mdpi.com/2075-4701/10/3/331.

Bosch, J., Staffell, I., Hawkes, A.D., 2018. Temporally explicit and spatially resolved global offshore wind energy potentials. Energy 163, 766–781. http://dx.doi.org/10.1016/j.energy.2018.08.153.

Cavaliere, P., 2019. Direct reduced iron: most efficient technologies for greenhouse emissions abatement. In: Clean Ironmaking and Steelmaking Processes. Springer International Publishing, Cham, pp. 419–484. http://dx.doi.org/10.1007/978-3-030-21209-4_8.

Chase, M., 1998. NIST-JANAF Thermochemical Tables, 4 9, American Chemical Society;American institute of Physics for the National institute of standards and technology, p. 1961,

Christensen, A., 2020. Assessment of hydrogen production costs from electrolysis: united states and Europe. URL:.

da Costa, A.R., Wagner, D., Patisson, F., 2013. Modelling a new, low CO2 emissions, hydrogen steelmaking process. J. Cleaner Prod. 46, 27–35. http://dx.doi.org/10.1016/J.JCLEPRO.2012.07.045, URL: https://www.sciencedirect.com/science/article/pii/S0959652612003836.

David, M., Ocampo-Martínez, C., na, R.S.-P., 2019. Advances in alkaline water electrolyzers: A review. J. Energy Storage 23, 392–403. http://dx.doi.org/10.1016/j.est.2019.03.001, URL: https://linkinghub.elsevier.com/retrieve/pii/S2352152X18306558.

DEA, 2020. Technology descriptions and projections for long term energy system planning. p. 234, Danish energy agency, URL: http://www.ens.dk/teknologikatalog.

Duarte, P., Pauluzzi, D., 2019. Premium quality DRI products from ENERGIRON. pp. 1–19, URL: https://www.energiron.com/wp-content/uploads/2019/05/Premium-Quality-DRI-Products-from-ENERGIRON.pdf Energiron.

EC, 2020. Report from the commission to the European parliament and the council, report on the functioning of the European carbon market. European Commission, Brussels, URL: https://eur-lex.europa.eu/legal-content/EN/TXT/?uri=CELEX%3A52020DC0740.

Elberry, A.M., Thakur, J., Santasalo-aarnio, A., 2021. Large-scale compressed hydrogen storage as part of renewable electricity storage systems. Int. J. Hydrogen Energy 46, 15671–15690. http://dx.doi.org/10.1016/j.ijhydene.2021.02.080.

Energiron, 2022. Hytemp -ENERGIRON hot metal transport. URL: https://www.energiron.com/hytemp-system/.

Equinor, 2021. Sse thermal and equinor developing plans for world-leading hydrogen storage facility in yorkshire. p. 1, URL: https://www.equinor.com/en/where-we-are/united-kingdom/sse-thermal-and-equinor-developing-plans-for-world-leading-hydrogen-storage-facility-in-yorkshire.html.

EUROFER, 2020. European steel in figures 2020. p. 74, EUROFER, URL: https://www.eurofer.eu/assets/Uploads/European-Steel-in-Figures-2020.pdf.

Fischedick, M., Marzinkowski, J., Winzer, P., Weigel, M., 2014. Techno-economic evaluation of innovative steel production technologies. J. Cleaner Prod. 84, 563–580. http://dx.doi.org/10.1016/j.jclepro.2014.05.063.

Gharghabi, S., Ding, Y., Yeh, C.C.M., Kamgar, K., Ulanova, L., Keogh, E., 2017. Matrix profile VIII: Domain agnostic online semantic segmentation at superhuman performance levels. In: Proceedings - IEEE International Conference on Data Mining. ICDM, 2017-Novem, pp. 117–126. http://dx.doi.org/10.1109/ICDM.2017.21.

Gielen, D., Saygin, D., Taibi, E., Birat, J.-P., 2020. Renewables-based decarbonization and relocation of iron and steel making: A case study. J. Ind. Ecol. 24, 1113–1125. http://dx.doi.org/10.1111/jiec.12997, URL: https://onlinelibrary.wiley.com/doi/10.1111/jiec.12997.

Gruobi, 2021. Gurobi optimizer reference manual.

Gulcin, D., Weber, N., Heinrichs, H.U., Linßen, J., Robinius, M., Kukla, P.A., Stolten, D., 2020. Technical potential of salt caverns for hydrogen storage in Europe. Int. J. Hydrogen Energy 45, 6793–6805. http://dx.doi.org/10.1016/j.ijhydene.2019.12.161.

Hampp, J., Düren, M., Brown, T., 2021. Import options for chemical energy carriers from renewable sources to Germany import options for chemical energy carriers from renewable sources to Germany.

Heidari, A., Niknahad, N., Iljana, M., Fabritius, T., 2021. A review on the kinetics of iron ore reduction by hydrogen. Materials 14, 7540. http://dx.doi.org/10.3390/ma14247540, URL: https://www.mdpi.com/1996-1944/14/24/7540.

Herman, J., Usher, W., 2017. SALib: An open-source Python library for sensitivity analysis. J. Open Source Softw. 2, 97. http://dx.doi.org/10.21105/joss.00097.

Howarth, R.W., Jacobson, M.Z., 2021. How green is blue hydrogen? Energy Sci. Eng. 1–12. http://dx.doi.org/10.1002/ese3.956.

Hunter, J.D., 2007. Matplotlib: A 2D graphics environment. Comput. Sci. Eng. 9, 90–95. http://dx.doi.org/10.1109/MCSE.2007.55.

Iberdola, 2022. Compressed hydrogen storage tanks. URL: https://www.iberdrola.com/press-room/news/detail/storage-tanks-green-hydrogen-puertollano.

IEA, 2020. Iron and steel technology roadmap : Towards more sustainable steelmaking. 3, p. 190,

IEA, 2021. IEA (2021) global energy review 2021, IEA, Paris. URL: https://www.iea.org/reports/global-energy-review-2021.

IRENA, 2020. Green hydrogen cost reduction: Scaling up electrolysers to meet the 1.5c climate goal. p. 106, IRENA, Abu Dhabi.

IRENA, 2022. Geopolitics of the energy transformation: The hydrogen factor. International Renewable Energy Agency.

Jacobasch, E., Herz, G., Rix, C., Müller, N., Reichelt, E., Jahn, M., Michaelis, A., 2021. Economic evaluation of low-carbon steelmaking via coupling of electrolysis and direct reduction. J. Cleaner Prod. 328, 129502. http://dx.doi.org/10.1016/j.jclepro.2021.129502, URL: https://linkinghub.elsevier.com/retrieve/pii/S0959652621036817.

Kim, S.H., Zhang, X., Ma, Y., Filho, I.R.S., Schweinar, K., Angenendt, K., Vogel, D., Stephenson, L.T., El-Zoka, A.A., Mianroodi, J.R., Rohwerder, M., Gault, B., Raabe, D., 2021. Influence of microstructure and atomic-scale chemistry on the direct reduction of iron ore with hydrogen at 700° c. Acta Mater. 212, http://dx.doi.org/10.1016/j.actamat.2021.116933.

Kirschen, M., Badr, K., Pfeifer, H., 2011. Influence of direct reduced iron on the energy balance of the electric arc furnace in steel industry. Energy 36, 6146–6155. http://dx.doi.org/10.1016/j.energy.2011.07.050.

Krüger, A., Andersson, J., Grönkvist, S., Cornell, A., 2020. Integration of water electrolysis for fossil-free steel production. Int. J. Hydrogen Energy http://dx.doi.org/10.1016/j.ijhydene.2020.08.116.

Levi, P., m'barek, B.B., Lu, H., Tao, J.Y., Xiuping, L., Swalec, C., Myllyvirta, L., Hasanbeigi, A., Zhang, Q., 2022. Global steel production costs. Transition zero, URL: https://www.transitionzero.org/reports/global-steel-production-costs.

LKAB, 2017. Lkab pellet steel vs. average European primary steel methodological appendix. URL: https://www.lkab.com/sv/SysSiteAssets/documents/blandat/lkab-value-chain-comparison-methodological-annex.pdf.

Lord, A.S., Kobos, P.H., Borns, D.J., 2014. Geologic storage of hydrogen: Scaling up to meet city transportation demands. Int. J. Hydrogen Energy 39, 15570–15582. http://dx.doi.org/10.1016/j.ijhydene.2014.07.121, URL: https://linkinghub.elsevier.com/retrieve/pii/S0360319914021223.

Maggiolino, S., 2019. Hyl newsletter 2019. URL: www.tenova.comandwww.energiron.com.

Matute, G., Yusta, J., Correas, L., 2019. Techno-economic modelling of water electrolysers in the range of several MW to provide grid services while generating hydrogen for different applications: A case study in Spain applied to mobility with FCEVs. Int. J. Hydrogen Energy 44, 17431–17442. http://dx.doi.org/10.1016/j.ijhydene.2019.05.092, URL: https://linkinghub.elsevier.com/retrieve/pii/S0360319919319482.

McKinney, W., 2010. Data structures for statistical computing in python. In: van der Walt, S., Millman, J. (Eds.), Proceedings of the 9th Python in Science Conference. pp. 51–56.

Midrex, 2021. Midrex hotlink process. URL: https://www.kobelco.co.jp/english/products/ironunit/dri/dri04.html.

Moro, A., Lonza, L., 2018. Electricity carbon intensity in European member states: Impacts on GHG emissions of electric vehicles. Transp. Res. D: Transp. Environ. 64, 5–14. http://dx.doi.org/10.1016/j.trd.2017.07.012.

nelhydrogen, 2022. Nel electrolysers-brochure. URL: https://nelhydrogen.com/product/atmospheric-alkaline-electrolyser-a-series/.

Nguyen, T., Abdin, Z., Holm, T., Mérida, W., 2019. Grid-connected hydrogen production via large-scale water electrolysis. Energy Convers. Manage. 200, 112108. http://dx.doi.org/10.1016/j.enconman.2019.112108, URL: https://www.sciencedirect.com/science/article/pii/S0196890419311148.

Nordpool, 2020. Nordpool historical electricity spot prices. URL: https://www.nordpoolgroup.com/historical-market-data/.

Norway, S., 2021. Statistics Norway. URL: https://www.ssb.no/en/energi-og-industri/energi/statistikk/elektrisitet.

OECD, 2020. Steel market developments Q2 2020. OECD, URL: https://www.oecd.org/sti/ind/steel-market-developments-Q2-2020.pdf.

Papadias, D.D., Ahluwalia, R.K., 2021. Bulk storage of hydrogen. Int. J. Hydrogen Energy 46, 34527–34541. http://dx.doi.org/10.1016/j.ijhydene.2021.08.028.

Pei, M., Petäjäniemi, M., Regnell, A., Wijk, O., 2020. Toward a fossil free future with hybrit: Development of iron and steelmaking technology in Sweden and Finland. Metals 10, 1–11. http://dx.doi.org/10.3390/met10070972.

Penev, M., Zuboy, J., Hunter, C., 2019. Economic analysis of a high-pressure urban pipeline concept (HyLine) for delivering hydrogen to retail fueling stations. Transp. Res. D: Transp. Environ. 77, 92–105. http://dx.doi.org/10.1016/j.trd.2019.10.005, URL: https://www.sciencedirect.com/science/article/pii/S1361920918311982.

Perez, F., Granger, B.E., 2007. IPython: A system for interactive scientific computing. Comput. Sci. Eng. 9, 21–29. http://dx.doi.org/10.1109/MCSE.2007.53.

Pimm, A.J., Cockerill, T.T., Gale, W.F., 2021. Energy system requirements of fossil-free steelmaking using hydrogen direct reduction. J. Cleaner Prod. 312, http://dx.doi.org/10.1016/j.jclepro.2021.127665.

Primemetals, 2022. Zero-carbon hyfor direct-reduction pilot plant starts operation. URL: https://magazine.primetals.com/2021/06/24/zero-carbon-hyfor-direct-reduction-pilot-plant-commences-operation-in-donawitz-austria/.

Rissman, J., Bataille, C., Masanet, E., Aden, N., Morrow, W.R., Zhou, N., Elliott, N., Dell, R., Heeren, N., Huckestein, B., Cresko, J., Miller, S.A., Roy, J., Fennell, P., Cremmins, B., Blank, T.K., Hone, D., Williams, E.D., de la Rue du Can, S., Sisson, B., Williams, M., Katzenberger, J., Burtraw, D., Sethi, G., Ping, H., Danielson, D., Lu, H., Lorber, T., Dinkel, J., Helseth, J., 2020. Technologies and policies to decarbonize global industry: Review and assessment of mitigation drivers through 2070. Appl. Energy 266, 114848. http://dx.doi.org/10.1016/j.apenergy.2020.114848.

Sartor, O., Sourrisseau, S., Mari, E., Peter, F., Buck, M., Graf, A., Vangenechten, D., 2022. Getting the transition to CBAM right: Finding pragmatic solutions to key implementation questions IMPULSE.

Sch, N., Bau, U., Reuter, M.A., Dahmen, M., Fritz, T.C.R., 2021. Decarbonizing copper production by power-to-hydrogen : A techno- economic analysis. J. Cleaner Prod. 306, http://dx.doi.org/10.1016/j.jclepro.2021.127191.

Schäfer, M., 2021. From 2025: “green” steel for Mercedes-Benz. URL: https://www.daimler.com/sustainability/climate/green-steel.html.

Sobol, I., 2001. Global sensitivity indices for non-linear mathematical models and their Monte carlo estimates. Math. Comput. Sumul. 5, 271–280.

Stöckl, F., Schill, W.P., Zerrahn, A., 2021. Optimal supply chains and power sector benefits of green hydrogen. Sci. Rep. 11, 1–14. http://dx.doi.org/10.1038/s41598-021-92511-6.

Stougaard, A., 2021. Ørsted joins the SteelZero initiative to support transition to low-carbon steel. URL: https://orsted.com/en/media/newsroom/news/2020/12/633975720078575.

Suer, J., Traverso, M., Ahrenhold, F., 2021. Carbon footprint of scenarios towards climate-neutral steel according to ISO 14067. J. Cleaner Prod. 318, 128588. http://dx.doi.org/10.1016/j.jclepro.2021.128588.

sunfire, 2022. Sunfire-hylink alkaline electrolyzer. URL: https://www.sunfire.de/files/sunfire/images/content/Sunfire.de%20(neu)/Sunfire-Factsheet-HyLink-Alkaline-20210305.pdf.

Sydvaranger, 2022. Norwegian Iron ore mine in northern Norway. URL: https://www.sydvarangergruve.no/home-eng.

Thomassen, G., Dael, M.V., Passel, S.V., You, F., 2019. How to assess the potential of emerging green technologies? Towards a prospective environmental and techno-economic assessment framework. Green Chem. 21, 4868–4886. http://dx.doi.org/10.1039/c9gc02223f.

thyssenkrupp, 2022. Thyssenkrupp electrolyzer brochure. URL: https://ucpcdn.thyssenkrupp.com/_binary/UCPthyssenkruppBAISUhdeChlorineEngineers/en/products/water-electrolysis-hydrogen-production/210622-gH2-product-brochure.pdf.

TianjinMainlandHydrogenEquipment, 2022. Tianjin mainland hydrogen equipment brochure. URL: http://www.cnthe.com/en/product_detail-35-43-30.html.

Towler, R.S.G., 2013. Chemical Engineering Design, second ed. Elsevier, http://dx.doi.org/10.1016/C2009-0-61216-2.

Trollip, H., McCall, B., Bataille, C., 2022. How green primary iron production in South Africa could help global decarbonization. Climate Policy 1–12. http://dx.doi.org/10.1080/14693062.2021.2024123.

UNCTAD, 2021. A European union carbon border adjustment mechanism : Implications for developing countries. United Nations Conference on Trade and Development, URL: https://unctad.org/system/files/official-document/osginf2021d2_en.pdf.

UNIDO, 2021. Industrial deep decarbonisation initiative. URL: https://www.unido.org/IDDI.

Uribe-Soto, W., Portha, J.-F., Commenge, J.-M., Falk, L., 2017. A review of thermochemical processes and technologies to use steelworks off-gases. Renew. Sustain. Energy Rev. 74, 809–823. http://dx.doi.org/10.1016/j.rser.2017.03.008, URL: https://linkinghub.elsevier.com/retrieve/pii/S1364032117303234.

V, M., Zhai, P., Pirani, A., Connors, S.L., Péan, C., Berger, S., Caud, N., Chen, Y., Goldfarb, L., Gomis, M.I., Huang, M., Leitzell, K., Lonnoy, E., Matthews, J., Maycock, T.K., Waterfield, T., Yelekçi, O., Yu, R., Zhou, B., 2021. Ipcc,2021: Climate change 2021: The physical science basis. contribution of working group I to the sixth assessment report of the intergovernmental panel on climate change. Cambridge University Press.

Vartiainen, E., Breyer, C., Moser, D., Medina, E.R., Busto, C., Masson, G., Bosch, E., Jäger-Waldau, A., 2021. True cost of solar hydrogen. Solar RRL http://dx.doi.org/10.1002/solr.202100487.

Vogl, V., Åhman, M., Nilsson, L.J., 2018. Assessment of hydrogen direct reduction for fossil-free steelmaking. J. Cleaner Prod. 203, 736–745. http://dx.doi.org/10.1016/j.jclepro.2018.08.279.

Vogl, V., Åhman, M., Nilsson, L.J., 2021a. The making of green steel in the EU: a policy evaluation for the early commercialization phase. Climate Policy 21, 78–92. http://dx.doi.org/10.1080/14693062.2020.1803040, URL: https://www.tandfonline.com/doi/full/10.1080/14693062.2020.1803040.

Vogl, V., Sanchez, F., Gerres, T., Lettow, F., Bhaskar, A., Swalec, C., Mete, G., Åhman, M., Lehne, J., Schenk, S., Witecka, W., Olsson, O., Rootzén, J., 2021b. Green steel tracker. URL: https://www.sei.org/featured/green-steel-tracker/.

Volvo, 2021. Volvo group and SSAB to collaborate on the world’s first vehicles of fossil-free steel. URL: https://www.volvogroup.com/en/news-and-media/news/2021/apr/news-3938822.html.

Wagner, M., 2009. Thermal analysis in practice. Collect. Appl. Thermal Anal..

Walt, S.V.D., Colbert, S.C., Varoquaux, G., 2011. The numPy array: A structure for efficient numerical computation. Comput. Sci. Eng. 13, 22–30. http://dx.doi.org/10.1109/MCSE.2011.37.

Weigel, M., Fischedick, M., Marzinkowski, J., Winzer, P., 2016. Multicriteria analysis of primary steelmaking technologies. J. Cleaner Prod. 112, 1064–1076. http://dx.doi.org/10.1016/j.jclepro.2015.07.132.

Wich, T., Lueke, W., Deerberg, G., Oles, M., 2020. Carbon2chem®-CCU as a step toward a circular economy. Front. Energy Res. 7, http://dx.doi.org/10.3389/fenrg.2019.00162, URL: https://www.frontiersin.org/article/10.3389/fenrg.2019.00162/full.

Worldsteel, A., 2020. Major steel-producing countries 2018 and 2019 million. pp. 1–8, 2020 World Steel in Figures, Worldsteel Association, URL: http://www.worldsteel.org/wsif.php.

YARA, 2021. Green ammonia from HEGRA to secure Norwegian competitiveness. URL: https://www.yara.com/corporate-releases/green-ammonia-from-hegra-to-secure-norwegian-competitiveness/.

Yeh, C.C.M., Zhu, Y., Ulanova, L., Begum, N., Ding, Y., Dau, H.A., Silva, D.F., Mueen, A., Keogh, E., 2017. Matrix profile I: All pairs similarity joins for time series: A unifying view that includes motifs, discords and shapelets. In: Proceedings - IEEE International Conference on Data Mining, ICDM. IEEE, pp. 1317–1322. http://dx.doi.org/10.1109/ICDM.2016.89.

Yeh, C.-C.M., Zhu, Y., Ulanova, L., Begum, N., Ding, Y., Dau, H.A., Zimmerman, Z., Silva, D.F., Mueen, A., Keogh, E., 2018. Time series joins, motifs, discords and shapelets: a unifying view that exploits the matrix profile. Data Min. Knowl. Discov. 32, 83–123. http://dx.doi.org/10.1007/s10618-017-0519-9.